



14<sup>TH</sup> CANADIAN MASONRY SYMPOSIUM  
MONTREAL, CANADA  
MAY 16<sup>TH</sup> – MAY 20<sup>TH</sup>, 2021



---

**NOVEL SOLAR REFLECTANCE TESTING METHOD AND CHARACTERIZATION OF  
MASONRY SAMPLES BASED ON COLOR AND SURFACE ROUGHNESS**

**Lentz, Theodore<sup>1</sup>, Huygen, Nathaniel<sup>2</sup> and Sanders, John<sup>3</sup>**

**ABSTRACT**

Solar reflectance is an important property for any building material because it dictates the thermal energy absorbed from solar radiation. An increase or decrease in thermal energy entering the building could increase energy consumption from HVAC units depending upon the local climate. There are many ASTM methods that can be utilized to measure solar reflectance. However, some of these test methods can be problematic to use due to limitations in their testing procedure. Testing completed using direct exposure to the sun have a limited time window for testing, are affected by current weather conditions, and require a large sample. Testing using portable solar reflectometers have a limited number of detectors, leading to an incomplete representation of infrared solar reflectance. To avoid some of these potential limitations a novel solar reflectance testing method was developed. This testing method uses a hot box apparatus to promote uniform boundary conditions and a calibrated infrared camera to measure the surface temperature of the sample. This method also uses a solar simulating light that is applied to the exterior surface of the sample. The energy absorbed from the light by the sample is then determined using an energy balance equation. This allows the solar reflectance to be measured based on surface temperature as opposed to the magnitude of reflected light. Several commercial bricks with varying colors and surface textures were characterized using this testing method. This was done to determine the relationship and correlation between the two properties and the solar reflectance. Testing has shown that darker colors or rougher surface textures result in lower solar reflectance values. Testing with this method has shown that changes in surface roughness can result in up to a 9% change in total solar reflectance.

**KEYWORDS:** *solar reflectance, surface roughness, color, hot box apparatus*

---

<sup>1</sup> Graduate Research Assistant, National Brick Research Center, 100 Clemson Research Blvd, Anderson, SC 29625, United States, [telentz@g.clemson.edu](mailto:telentz@g.clemson.edu)

<sup>2</sup> Research Assistant, National Brick Research Center, 100 Clemson Research Blvd, Anderson, SC 29625, United States, [nhuygen@clemson.edu](mailto:nhuygen@clemson.edu)

<sup>3</sup> Director, National Brick Research Center, 100 Clemson Research Blvd, Anderson, SC 29625, United States, [jpsand@clemson.edu](mailto:jpsand@clemson.edu)

## **INTRODUCTION**

The solar reflectance of the building envelope and roof are important factors to consider when constructing a building. As of 2009, within the United States, the climate control within a residential building accounts for approximately 47.7% of the total energy consumption [1]. Altering the heat flux entering the building by optimizing the solar reflectance of any given wall system will result in decreased energy consumption. The optimal solar reflectance is dependant upon both the properties of the building envelope and the local climate. The importance of solar reflectance has also been reaffirmed within ASHRAE building standards. Any building envelope within Climate Zone 0 is required to have an SRI of 29 or higher or have 30% of the surrounding wall covered in shade by the surrounding landscape [2]. Assuming the material has an emissivity of 0.8-0.9 which is common for ceramics and masonry materials, the solar reflectance would be approximately 30% for an SRI of 29. This severely limits the uses of certain bricks, particularly darker colored bricks, and places the common red brick on the threshold of acceptance with a typical solar reflectance of approximately 34%. While Climate Zone 0 is not within the continental United States, there are similar limitations on the SRI of roofs that extend into Climate Zone 2 [2]. If the SRI requirements for building envelopes were to be extended to match the requirements for roofs and include Climates Zones 1 and 2 then the aesthetic choices for brick veneer in the southern United States would be limited.

There are several ways to determine the solar reflectance of a sample. Testing can traditionally be completed following ASTM E1918, ASTM C1549, or ASTM E903. Each of these testing methods have their benefits and drawbacks depending on the precision, sample preparation, test duration and cost. ASTM E1918 requires a 4 meter in diameter sample and a clear, cloudless day within 2-3 hours of solar noon [3]. Testing conducted using ASTM C1549 only measures four unique wavelengths to determine the solar reflectance of a sample [4]. These measurements are at 380, 500, 650, and 1220 nm limiting the representation of the infrared reflectance [4]. Testing conducted using ASTM E903 has already overcome the limitations of the previously mentioned ASTM testing methods but is quite expensive as it employs the use of a spectrophotometer. Also, ASTMs C1549 and E903 both have limitations regarding the extreme surface roughness of the sample due to the apparatus requiring having suitable contact with the surface [4, 5].

The novel test method, however, measures the surface temperature of the sample as a result of its solar absorption. This testing method utilizes smaller samples and considers the entire solar spectrum. There are two main surface properties that can alter the solar reflectance of a material that the novel solar reflectance test will help to characterize: color and surface roughness [6, 7].

## **NOVEL SOLAR REFLECTANCE TESTING METHOD**

The novel solar reflectance test is conducted within a small-scale hot box apparatus. The interior of both chambers are monitored using thermocouples and humidity sensors to properly account for environmental conditions. Air is circulated using fans to promote a uniform surface temperature during testing. The climatic side houses the light source and is representative of the

external environment while the metering side is representative of an internal environment. As can be seen in Figure 1 the climatic side and sample holder are also painted white to prevent the box from absorbing excess light. The metering side of the small-scale hot box was modified to include an infrared camera for noncontact measurement of the sample during testing.



**Figure 1: Small Scale Hot Box climatic (right), exterior, and metering (left) view**

The novel test method operates by utilizing a heat balance equation. This implies that after the sample has reached steady state heat transfer that the energy leaving the sample is equal to the energy entering the sample. A visual representation of the heat flow is shown in Figure 2 demonstrating the energy entering and leaving the sample. The heat flow equations are also listed in Equations 1-4. Where the environmental variables  $h_c$  [ $\text{W}/\text{m}^2$ ],  $T_c$  [K],  $T_m$  [K] represent the convective coefficient of air, the climatic air temperature, and the metering side temperature, respectively. The sample variables  $\varepsilon$  [-],  $k_s$  [ $\text{W}/\text{K}$ ],  $T_{s,c}$  [K],  $T_{s,m}$  [K], and  $R$  [ $\text{K}/\text{W}$ ] represent the thermal emissivity, thermal conductivity, surface temperature on the climatic side, surface temperature on the metering side, and thermal resistivity of the sample. The remaining variables  $q_m$  [ $\text{W}/\text{m}^2$ ],  $q_c$  [ $\text{W}/\text{m}^2$ ],  $q_{abs}$  [ $\text{W}/\text{m}^2$ ],  $\sigma$  [ $\text{J}/\text{K}$ ], and  $\Delta T$  [K] represent the heat flow into the metering side, the heat flow into the climatic side, the total heat loss from the sample, Boltzmann's constant, and the temperature gradient through the sample.

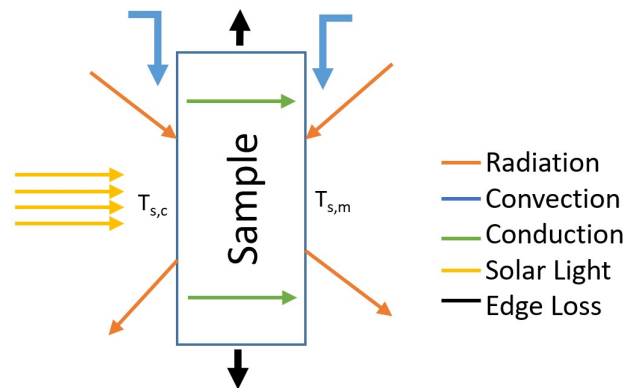


**Figure 2: Schematic of Heat Flow Through the Sample**

$$q_m = h_c (T_{s,m} - T_m) + \epsilon \sigma (T_{s,m}^4 - T_m^4) \quad (1)$$

$$q_c = h_c (T_{s,c} - T_c) + \epsilon \sigma (T_{s,c}^4 - T_c^4) \quad (2)$$

$$q_{abs} = q_c + q_m \quad (3)$$

$$R = \frac{\Delta T}{q_m} = \frac{thickness}{k_s} \quad (4)$$

Before solar reflectance testing  $\epsilon$  and  $k_s$  are measured for each sample. During testing the infrared camera records  $T_{s,m}$  and the thermocouples record  $T_c$ ,  $T_m$  in both testing chambers. The variables  $h_c$  has been estimated from prior characterization of the small hot box apparatus. Using the known variables,  $q_m$  can be determined from Equation 1. Then using  $q_m$ ,  $\Delta T$  can be derived from Equation 4. Knowing  $\Delta T$  allows  $T_{s,c}$  to be derived which is then used in Equation 2 to evaluate  $q_c$ . Finally, with both  $q_m$  and  $q_c$ ,  $q_{abs}$  can be found using Equation 3. Since the system is at steady state,  $q_{abs}$  is equal to the absorbed energy from the solar mimicking light. The only heat flow not recorded or calculated is the edge loss from the sample. It is not possible to calculate this heat loss, but it is accounted for in the calibration.

The test method was calibrated using samples tested by a third party following the methods outlined in ASTM C1549. There were four samples: black, red, buff, and white that were used as calibration samples to provide a range of solar reflectance values. Having an enclosed testing environment allowed for light to encounter the sample multiple times after being reflected off the interior of the box. This required the inclusion of a multiscattering variable in the calibration equation. Another variable ( $a$ ) was also included to represent any unaccounted heat transfer such as edge loss or heating from the light source. The calibration equation was derived by an equation for reflectance considering the probability of multiscattering [7] and can be found in Equation 5. In Equation 5 the variables SR [-],  $Q_0$  [W/m<sup>2</sup>],  $Q$  [W/m<sup>2</sup>], and  $p$  [-] represent the solar reflectance, initial heat flux, measured heat flux, and probability of multiscattering.

$$SR = \frac{1 - p}{\frac{Q_0}{Q - a} - p} \quad (5)$$

This results in a very low testing error provided the thermal emissivity and thermal conductivity are both known. There was also a low standard deviation between tests conducted on samples made of the same materials. The novel solar reflectance test has an average standard deviation of approximately 1.8% and a testing error of approximately 0.5% making the test both repeatable and accurate.

### ***Light Source***

The light source selected for this test method was a xenon arc light. Several light sources were considered including the xenon arc light, LED, and incandescent lighting. The incandescent light source was eliminated from consideration as it released an abundance of infrared light. Conversely the LED light did not emit enough infrared light as it was limited in the range of wavelengths that it could emit. LED light sources can properly mimic solar light up until approximately 1100nm [8]. However, according to ASTM G173-03 most of the solar spectrum exists between the wavelengths of 300-2500nm [9]. Having the measured range stop at 1100nm would limit the measured solar reflectance and cut off a large portion of the infrared region. Xenon arc lights can emit light across the entire solar spectrum; however, there is an over representation from 800-1000 nm within the xenon arc light spectrum [8]. Both light sources are commonly accepted to represent AM1.5G, or the average global solar spectrum, with an associated optical filter, but a xenon arc light was used for the novel testing method because it fully represented the infrared region of the solar spectrum.

### **SAMPLES AND ANALYSIS**

The samples chosen for this study were manufactured brick with varying color and surface texture. These consisted of a brown, red, buff, and white colored samples. To analyze the effects of surface roughness, different surface finishes, smooth or rough, were tested for each sample color. These samples can be seen in Figure 3 along with their respective color and surface finish.

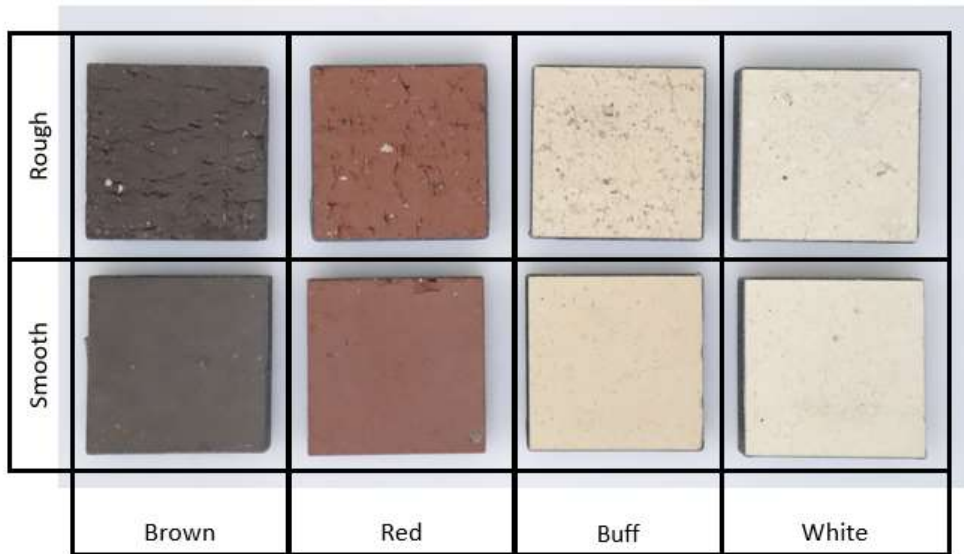


**Figure 3: Characterization Samples**

### ***Color***

It is well known that the color of a sample effects the solar reflectance. However, many studies focus on altering the surface to be white and measuring the resultant change in heat flux. One such study found that by resurfacing the roof and coloring it white the heat flux entering the building

was decreased by approximately 20% [6]. Another study that measured several different roofs in various conditions found that a recent white coating of paint can reduce the heat flux by 33-43% when compared to a corroded galvanized roof [10]. Another study conducted by Berdahl and Bretz showed a direct correlation between the  $L^*$  value and the solar reflectance of materials [11].

There are many ways to measure color. The two most common ways are RGB and CIE  $L^*$ ,  $a^*$ ,  $b^*$ . Using RGB to represent color when comparing color to solar reflectance is difficult. This is due to RGB being a measure of the primary colors red, blue, and green. However, CIE  $L^*$ ,  $a^*$ ,  $b^*$  color values are easier to compare to solar reflectance. Within  $L^*$ ,  $a^*$ , and  $b^*$  color values  $L^*$  is representative of the lightness of the color while  $a^*$  and  $b^*$  represent the hue of the color [12]. The system operates using the opposing color theory where  $a^*$  represent red and green while  $b^*$  represents yellow and blue [12]. With these two values determining the hue the  $L^*$  value describes the lightness from black to white. This allows for the  $L^*$  value to be directly correlated back to the solar reflectance. Solar reflectance is a function of lightness as it is a fundamental property in the solar reflectance index which is an unitless comparison of the thermal performance of a sample in direct solar radiation to a white and black sample [13].

There was found to be a clear correlation between lightness and solar reflectance as expected. The white sample was the most reflective followed by the buff, then red and finally the brown sample. The changes in color were shown to alter the solar reflectance by 50.9% from the lightest to the darkest measured samples. The data reported in Table 1 shows each of the samples and their recorded solar reflectance and  $L^*$  values.

**Table 1: Solar Reflectance and  $L^*$  values**

<b>Sample (Surface Treatment)</b>	<b>Solar Reflectance (%)</b>	<b><math>L^*</math></b>
Brown (Smooth)	21.5	34.3
Red (Smooth)	29.9	38.3
Buff (Smooth)	61.5	73.7
White (Smooth)	71.4	81.4
Brown (Rough)	14.7	34.1
Red (Rough)	27.5	36.9
Buff (Rough)	53.8	73.7
White (Rough)	71.4	81.6

When the  $L^*$  value is plotted against solar reflectance there was a linear trend that can be seen in Figure 4. There was scatter seen in the comparison for both rough samples and smooth samples; however, the scatter was more pronounced for the rough samples. The scatter was likely caused by surface roughness of the rough samples not being controlled or kept constant.

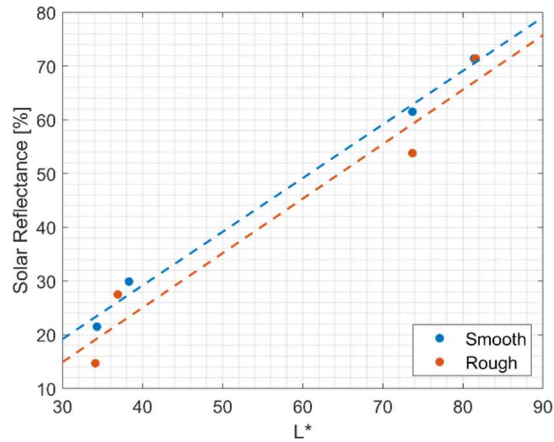


**Figure 4: L\* Value vs Solar Reflectance of Rough and Smooth Samples**

The correlation between L\* value and solar reflectance is given by Equation 6. The variable SR represent solar reflectance. A direct relationship between L\* value and solar reflectance can be seen in Equation 6. This indicates that a 1-unit change in L\* value is approximately equivalent to a 1% change in solar reflectance. The equation also provides a general prediction of solar reflectance based on the samples L\* value.

$$SR = 0.998L^* - 10.74 \quad (6)$$

### **SURFACE ROUGHNESS**

Surface roughness alters the solar reflectance of a sample by changing the probability of multiscattering [7]. As the surface roughness increases the topography of the sample develops more peaks and valleys that promote light to encounter the surface of the sample and then, after the light is reflected, encounter the surface of the sample again. This causes the sample to absorb a portion of the incident light multiple times. As a result, the reflectance of the sample would be a function of the micro-reflectance, or the reflectance of a perfectly smooth sample, and the probability that light will experience multiscattering [7].

In order to measure the effect of multiscattering, brick samples with two different surface finishes were analyzed. These samples were wirecut and die skin samples or the rough and smooth samples, respectively. The surface roughness for these samples was not controlled but it was measured. The surface roughness of each sample was measured using a Keyence VHX-6000 microscope and its 3D image stitching functionality. The reported Sa or average surface roughness was used to represent the surface roughness of each sample. These samples were also measured using a qualitative method of placing the samples under direct sunlight for several hours and measuring the surface temperature using an infrared camera. This was completed as a proof of concept as samples that were tested by an accredited third party using the process defined in ASTM C1549 found no significant difference in solar reflectance between the rough and smooth samples. The results for these tests can be seen in Table 2. This resulted in the necessity to confirm that surface

roughness did change the solar reflectance as both literature and the novel testing method suggested.

**Table 2: Solar Reflectance Values for Novel and ASTM C1549**

Sample (Surface Treatment)	Novel (%)	ASTM C1549 (%)
Buff (Rough)	61.5	62.2
Buff (Smooth)	53.8	62.4

To determine if surface roughness influenced the solar reflectance, selected samples were placed outside in direct solar light for several hours. The samples were placed on an insulating form board to minimize conduction from the ground into the samples. Also, as all samples were placed outside at the same time and measured simultaneously using an infrared camera each sample should have experienced identical environmental conditions. The resulting images are shown in Figure 5. The wirecut samples are on the bottom row with their smooth counterparts above them. A white and black tile were also placed at the far-right side as they were used as calibration standards for the novel test method.

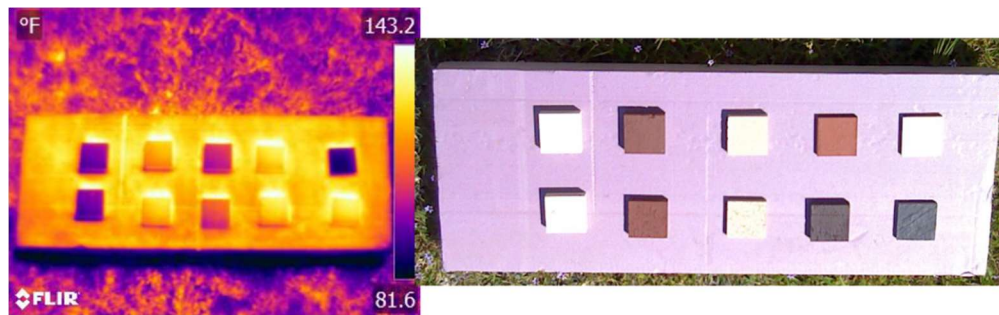


**Figure 5: Infrared Image (Left) and Visible Image (Right) of The Characterized Samples Under Direct Solar Radiation**

From the image it was determined that all the wirecut samples, except for the white samples, had higher surface temperatures implying that they had absorbed more thermal energy and had lower solar reflectance values. These samples and their solar reflectance values and surface temperatures are shown in Figure 6.

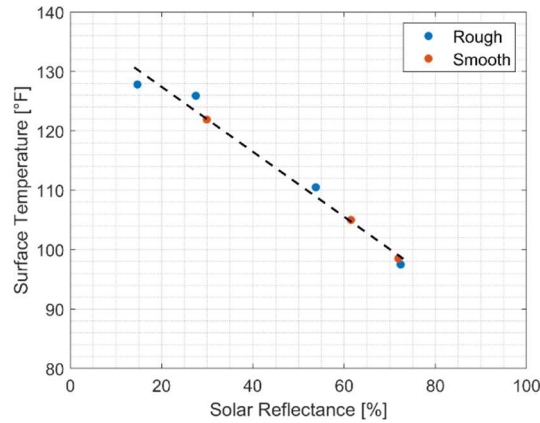


**Figure 6: Solar Reflectance vs Qualitative Surface Temperature**

The solar reflectance also varied significantly due to alterations in surface roughness when tested with the novel solar reflectance method. Each sample, other than the white samples, showed the surface roughness was higher for the rough sample and that the rough samples also had a lower solar reflectance. These trends are illustrated by the data in Table 4. The largest measured change in solar reflectance between smooth and rough samples was 7.7% total solar reflectance with one sample experiencing an approximately 46.3% change in relative solar reflectance due to a change in surface roughness.

**Table 4 : Solar Reflectance (SR) versus Surface Roughness (Sa)**

Sample Color	SR (%) Smooth	SR (%) Rough	Sa (µm) Smooth	Sa (µm) Rough
Brown	21.5	14.7	51.7	60.12
Red	29.9	27.5	26.23	81.38
Buff	61.5	53.8	30.34	82.46
White	71.9	72.4	37.25	23.93

### *Comparative Analysis*

When color and surface roughness are each compared to solar reflectance individually the resulting relationships appear to be roughly linear. The solar reflectance will decrease with a decrease in  $L^*$  value or an increase in surface roughness,  $S_a$ . Showing a direct relationship between  $L^*$  value and solar reflectance and an inverse relationship between surface roughness and solar reflectance. However, when these are analyzed together, the result is a linear plane that provides a general prediction of the solar reflectance based on the  $L^*$  value and  $S_a$  of the sample. The equation for this relationship, based on this studies data set, can be seen in Equation 7.

$$SR = 0.927L^* - 0.1115S_a - 1.94 \quad (7)$$

The data within Table 5 shows the predicted and measured solar reflectance for each of the analyzed samples. This prediction is usually within four percent of the measured solar reflectance value. The equation shows that the color or  $L^*$  value has a more drastic impact on solar reflectance

as compared to surface roughness, Sa. However, the surface roughness can have a significant impact on the relative solar reflectance for samples with lower L\* values.

**Table 5: Measured and Predicted Solar Reflectance Values**

<b>Sample Color</b>	<b>Measured Smooth (%)</b>	<b>Predicted Smooth (%)</b>	<b>Measured Rough (%)</b>	<b>Predicted Rough (%)</b>
Brown	21.5	24.1	14.7	23.0
Red	29.9	30.6	27.5	23.2
Buff	61.5	63.0	53.8	57.2
White	71.9	69.4	72.4	71.0

The relationship between the three variables is a curve fit for the data collected during the study. This results in a surface roughness range of approximately 20-80 micron and a L\* value range of approximately 30-80, and this equation is only valid over these ranges of values.

## **CONCLUSIONS**

The study illustrates that both color and surface roughness have a profound impact on the solar reflectance. Analysis also gave a defined relationship between color, specifically L\* value, and solar reflectance. The surface roughness was observed to result in a reduction in measured solar reflectance in both the novel test and the qualitative test. Results obtained from ASTM C1549 was also found to be insensitive to the effect of surface roughness. ASTM C1549 indicated a testing bias within the standard but the cause was unknown. This insensitivity to surface roughness could be the cause.

## **ACKNOWLEDGEMENTS**

Special thanks to the National Brick Research Center and Clemson University for funding and support on this research. We also give thanks to the industry sponsors who generously provided the samples that were tested in this study.

## **REFERENCES**

- [1] U.S. Energy Information Administration, "Heating and cooling no longer majority of U.S. home energy use," 7 March 2013. [Online]. Available: <https://www.eia.gov/todayinenergy/detail.php?id=10271>.
- [2] Standard 90.1, "Energy Standard for Buildings Except Low-Rise Residential Buildings," ASHRAE, Peachtree Corners, Georgia, 2019.
- [3] ASTM E1918-16, "Standard Test Method for Measuring Solar Reflectance of Horizontal and Low-Sloped Surfaces in the Field," ASTM International, West Conshohocken, PA, 2016.
- [4] ASTM C1549-16, "Standard Test Method for Determination of Solar Reflectance Near Ambient Temperature Using a Portable Solar Reflectometer," ASTM International, West Conshohocken, PA, 2016.

- [5] ASTM E903-20, "Standard Test Method for Solar Absorption, Reflectance, and Transmittance of Materials Using Integrating Spheres," ASMT International, West Conshohocken, PA, 2020.
- [6] D. S. Parker, J. R. Sherwin, J. K. Sonne and S. F. Barkaszi, "Demonstration of Cooling Savings of Light Colored Roof Surfacing in Florida Commercial Buildings: Our Savior's School," Florida Solar Energy Center, Cocoa, FL, 1996.
- [7] P. Berdahl, H. Akbari, J. Jacobs and F. Klink, "Surface roughness effects on the solar reflectance of cool asphalt shingles," *Solar Energy Materials and Solar Cells*, vol. 92, no. 4, pp. 482-489, 2008.
- [8] G. P. Leary, "Comparison of Xenon Lamp-Based and LED-Based Solar Simulators," Montana State University, Bozeman, Montana, April, 2016.
- [9] ASTM G173-03, "Standard Tables for Reference Solar Spectrum Irradiances: Direct Normal and Hemispherical on 37° Tilted Surface," ASTM International, West Conshohocken, PA, 2020.
- [10] H. Suehrcke, E. L. Peterson and N. Selby, "Effect of roof solar reflectance on the building heat gain in a hot climate," *Energy and Buildings*, vol. 40, pp. 2224-2235, 2008.
- [11] P. Berdahl and S. Bretz, "Preliminary survey of the solar reflectance of cool roofing materials," *Energy and Buildings*, vol. 25, pp. 149-158, 1997.
- [12] Hunter Associates Laboratory, "Measuring Color Using Hunter L, a, b versus CIE 1979 L\*a\*b\*," HunterLab, Reston, VA, 2012.
- [13] ASTM E1980-11, "Standard Practice for Calculating Solar Reflectance Index of Horizontal and Low-Sloped Opaque Surfaces," ASTM International, West Conshohocken, PA, 2019.
- [14] ASTM E1933-14, "Standard Practice for Measuring and Compensating for Emissivity Using Infrared Imaging Radiometers," ASTM International, West Conshohocken, PA, 2018.